Langmuir

Article

pubs.acs.org/Langmuir

Controlled Evaporative Self-Assembly of Poly(acrylic acid) in a Confined Geometry for Fabricating Patterned Polymer Brushes

Yonghong Men,[†,§] Peng Xiao,[†] Jing Chen,[*,†] Jun Fu,[†] Youju Huang,[†] Jiawei Zhang,[†] Zhengchao Xie,[‡] Wenqin Wang,[§] and Tao Chen[*,†]

[†]Division of Polymer and Composite Materials, Ningbo Institute of Material Technology and Engineering, Chinese Academy of Science, 519 Zhuangshi Road, Ningbo 315201, China

[‡]Faculty of Science and Technology, University of Macau, Macau, China

[§]Faculty of Materials Science and Chemical Engineering, Ningbo University, Ningbo 315211, China

ABSTRACT: A simple yet robust approach was exploited to fabricate large-scaled patterned polymer brushes by combining controlled evaporative self-assembly (CESA) in a confined geometry and self-initiated photografting and photopolymerization (SIPGP). Our method was carried out without any sophisticated instruments, free of lithography, overcoming current difficulties in fabricating polymer patterns by using complex instruments.

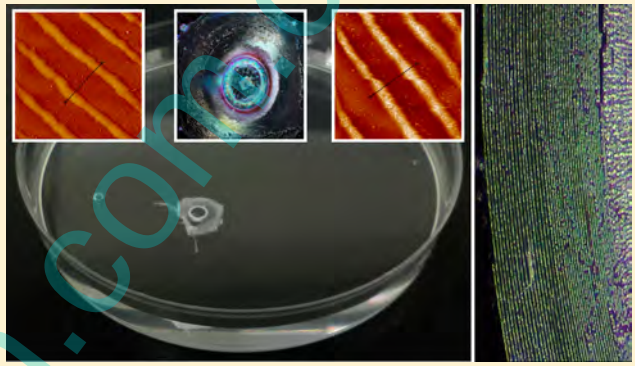

INTRODUCTION

Patterned polymer brushes play an important role in the modification of surface properties and have attracted considerable interest because of their potential applications in many surface-based technologies such as protein-resistant coatings, sensors, and substrates for cell-growth control.[1−3] They can be fabricated by chemical lithography,[4] microcontact printing (μCP),[5] electron-beam lithography (EBL),[6] electron-beam chemical lithography (EBCL),[7,8] and dip-pen nanodisplacement lithography (DNL),[9] etc. Among these methods, although μCP is a particularly simple and cost-effective tool to fabricate polymer brushes, the master preparation process still requires the expensive and complex UV lithographic instrument. Therefore, exploiting simpler strategies to fabricate polymer brush morphologies is still more desirable and remains a challenge.[2]

Recently, a method of the drying-mediated self-assembly via irreversible solvent evaporation of an unbound droplet solution containing nonvolatile solutes yielded intriguing complex patterns, which has attracted significant attention.[10−12] Although these patterns were created by the simple lithography and external field free means, they often lacked the regularity and high fidelity due to the flow instabilities within drying droplet. A rational preparation strategy has been developed to solve this problem through the controlled evaporative self-assembly (CESA) in a confined geometry. The existence of the confined geometry provides an optimal environment for controlling the evaporation process (e.g., evaporative flux, solution concentration, interfacial interaction between the solute and substrate, etc.),[13] so that we can create highly ordered patterns.

Some various geometries, such as two-plate geometry,[14] cylindrical tubes,[15] two-crossed cylinders,[16] evaporative lithography,[17] and curve-on-flat geometry,[18−22] have been successfully exploited for the CESA. Through this strategy, nanoparticles,[23] quantum dots,[19] polymers,[18,24−26] and graphene oxide,[27] etc., have been organized on the nanoscale into ordered microscopic structures over large surface areas.

In addition to growing polymer brushes from surface-confined initiators by surface initiated polymerization,[1] it was demonstrated recently that patterned polymer brushes can also be prepared even without a surface bound initiator by self-initiated photografting and photopolymerization (SIPGP) on photoactive patterned SAMs.[28−30] As various materials have been organized into patterned structures, this thus inspired us to find a much simpler strategy to construct photoactive patterns by CESA in a confined geometry for growing polymer brushes via SIPGP.

Herein, we represent a simple yet robust approach to fabricate patterned polymer brushes in a large scale, up to centimeter through SIPGP from the template of photoactive poly(acrylic acid) (PAA) films generated via CESA in a confined geometry of sphere-on-flat. The advantage of our approach is the exploitation of an existing, simple technology to

Received: March 14, 2014
Revised: April 3, 2014
Published: April 4, 2014

   dx.doi.org/10.1021/la500996a | *Langmuir* 2014, 30, 4863−4867

generate a photoactive template without the necessity of sophisticated instruments, which results in an advance in the generation of patterned polymer brushes after polymerization amplification.

EXPERIMENTAL SECTION

Materials and Sample Preparation. Polyacrylic acid (PAA, average molecular weight, M_w = 15 000) was selected as nonvolatile solute. The spherical lens made from fused silica (diameter 1 cm) and Si wafer were cleaned in the mixture of H_2O_2/H_2SO_4, 1:3 (v/v, i.e., "piranha solution") at 80 °C for 1 h. Subsequently, they were rinsed with deionized water extensively and blow-dried with N_2. Styrene was purified by neutral Al_2O_3 column and dried with a 0.4 nm molecular sieve at room temperature for 3 days.

Evaporative Self-Assembly of PAA Aqueous Solution.[19] A drop of PAA aqueous solution (10 μL) was loaded on the Si wafer, and then the spherical lens was brought into contact with Si substrate. The evaporation process was carried out in a sealed chamber and at room temperature. The use of a sealed chamber eliminated the possible external influences such as the humidity in an open space and air convection. The whole evaporation took about 4 h to complete. Afterward, the sphere and Si were separated, and the structures (e.g., concentric rings composed of PAA) were produced on Si surfaces.

Self-Initiated Photografting and Photopolymerization.[31] The patterned Si substrate was submerged in 2 mL of styrene and irradiated with an UV lamp with a spectrum between 300 and 400 nm (intensity maximum at λ = 350 nm with a total power of 9 mW/cm^2) for 1 h. Then, the substrate was exhaustively rinsed with different solvents (toluene, ethyl acetate, and ethanol) to remove physisorbed polymer.

Characterization. The concentric rings produced on Si substrate were characterized by optical microscopy (Olympus BX51) in the reflection mode and atomic force microscopy (CSPM 5500) in tapping mode. The spring constant of scanning probes is 40 N/m. Static water contact angles were measured at room temperature using the sessile drop method and image analysis of the drop profile. The instrument (OCA-20, Dataphysics) used a charge-coupled device (CCD) camera and an image analysis processor. The water (Milli-Q) droplet volume was 5 μL, and the contact angle was measured after the drop was stable on the sample. For each sample, the reported value is the average of the results obtained on three droplets.

RESULTS AND DISCUSSION

The procedure for constructing PAA pattern via CESA in a confined geometry and subsequent amplification of growing patterned polymer brushes is schematically shown in Figure 1. PAA aqueous solution was first loaded and trapped between the sphere and Si substrate (Figure 1A), which yielded a capillary-held solution. As the water evaporated, PAA was transported from the solution inside to the capillary edge and pinned at the contact line, thereby forming a coffee-ring like deposit (Figure 1B). Because of the imposed geometrical constraint, the evaporation was constrained to occur only at the droplet edge,[18,21,23] which in turn led to the formation of highly ordered concentric rings.[18] During the deposition process, the initial contact angle of the capillary edge decreased gradually to a critical angle due to continuous evaporative loss of water, at which the capillary force (depinning force) became larger than the pinning force.[32] This caused the contact line to jump to a new position, where it was pinned again and yielded a new ring. Consequently, the repetitive pinning and depinning (i.e., "stick–slip" motion) of the contact line led to the formation of gradient concentric rings of PAA (Figure 1C). The formation of gradient concentric rings was a direct consequence of the competition between the nonlinear capillary force from the curvature of the spherical droplet, and the linear pinning

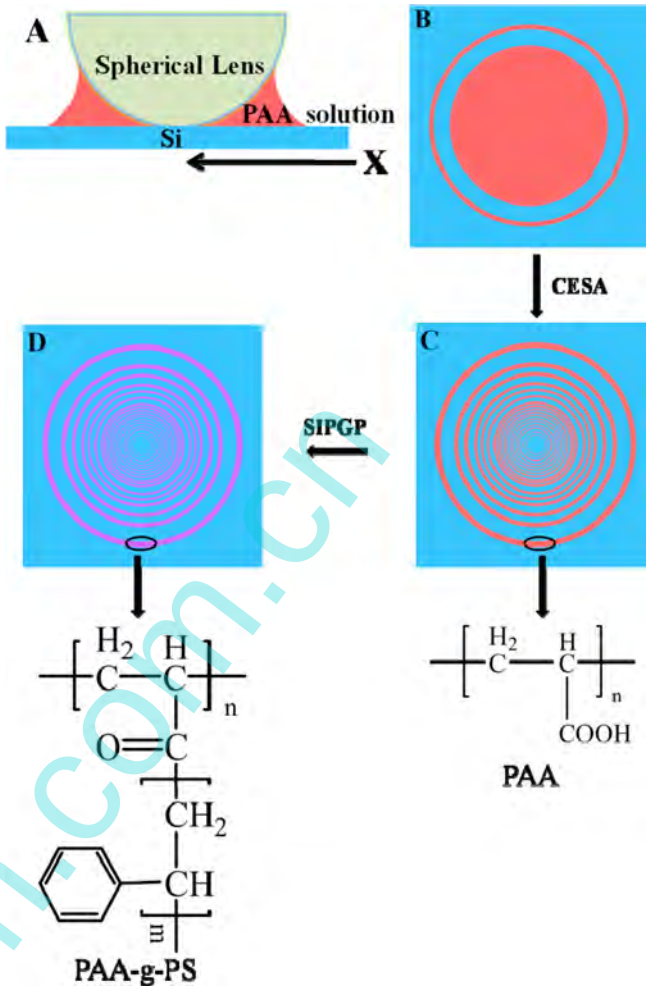

Figure 1. Schematic procedure of fabricating patterned polymer brushes via SIPGP by using the CESA induced template of PAA in a confined geometry. (A) Cross section of PAA solution confined in the sphere-on flat geometry. The distance between the concentric rings and the sphere/Si contact center is *Xn* (n = 1–3). (B, C) The process of CESA of PAA in the confined geometry. (D) Growing polymer brushes by SIPGP using PAA patterns generated by CESA.

force.[32] As a photoactive site, −COOH on PAA chains could be initiated to grow polymer brushes by SIPGP from patterned PAA rings without a surface-bonded initiator[28] (Figure 1D).

As a reasonably simple and convenient strategy, CESA could be used to organize almost all nonvolatile solutes into patterns. PAA, a very important polyelectrolyte with abundant active group in the polymer chain, has the potential to prepare functional materials after the subsequent functionalization upon the formation of well-organized patterns by CESA in a confined geometry. As proof-of-concept, we used PAA with an average molecular weight of M_w at 15 000 to generate this pattern by CESA. Figure 2A shows a typical optical microscopy image of highly ordered, microscopic PAA stripes on the Si substrate locally formed in the sphere-on-flat geometry. Our resultant PAA pattern is consistent with previous reports of patterns formed by CESA in a confined geometry.[33] Atomic force microscopy (AFM) was performed to further characterize the surface morphologies of the PAA rings. Two typical positions of the pattern, B and C in Figure 2A, were shown to prove the stripes were gradual in height and in distance (Figure 2B,C). From the AFM height images, it is worth noting that the

dx.doi.org/10.1021/la500996a | Langmuir 2014, 30, 4863–4867

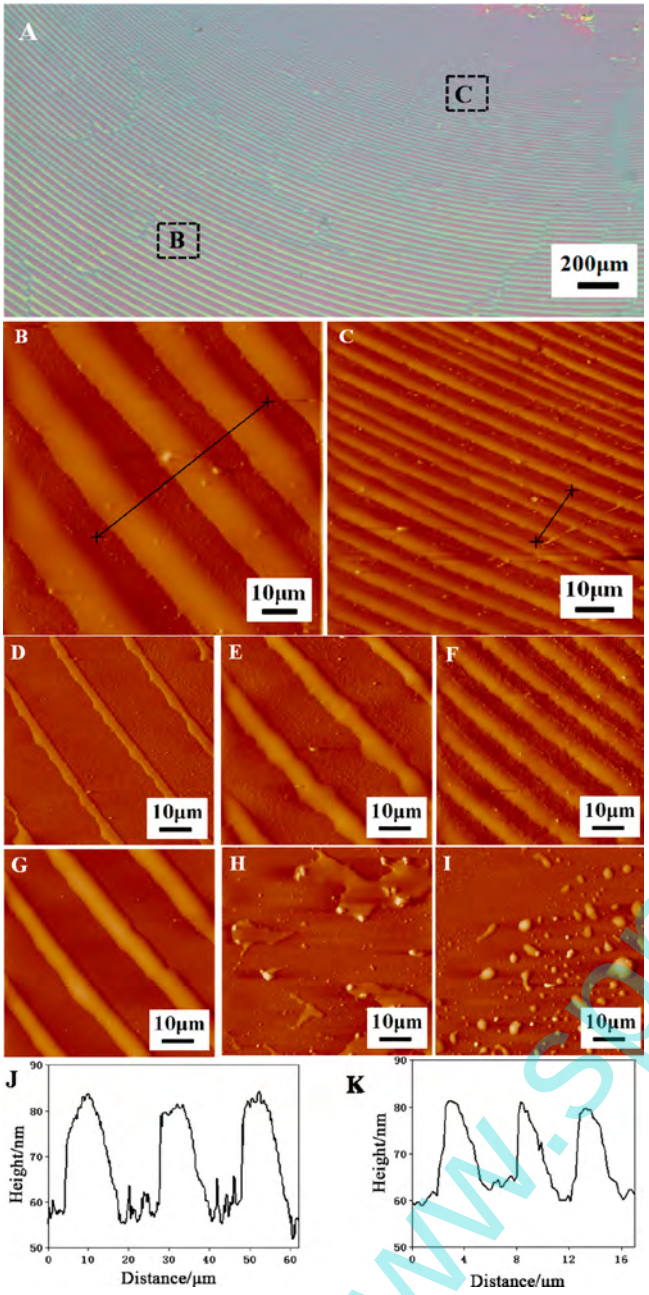

Figure 2. Optical micrograph images and AFM height images of gradient concentric PAA rings. The concentration is 0.2 mg/mL in panel B, C, G, H, and I; 0.05 mg/mL in panel D; 0.1 mg/mL in panel E; 0.4 mg/mL in panel F. The pH value is 1.0 in panel B, C, D, E and F; 3.0 in panel G; 5.0 in panel H; and 7.0 in panel I.

morphology parameters of the height, *H*, the width, *W*, of the concentric rings, and the center-to-center distance between neighboring PAA rings, *D*, decreased progressively as *X* (the distance of the concentric rings away from the sphere/Si contact center) gradually approached the sphere/Si contact center. At the outermost region, the *H*, and the *W*, and the *D* decreased progressively from H = 24 nm, W = 12 μm, D = 10 μm ($X_1 \approx$ 2100 μm) to 16 nm, 3 μm, and 3 μm at the innermost region ($X_2 \approx$ 1100 μm), as measured by AFM.

The morphology could also be adjusted by varying the concentration of PAA solution, which is shown in Figure 2 B,D–F (a similar characterization position with Figure 2B). It was found that concentric rings become denser upon increasing the concentration from 0.05 to 4 mg/mL. As a weak polyelectrolyte, PAA with the pK_a at 4.75 will have a various conformations, i.e., collapsed or swollen, at different pH values, which play an important role in the formation of PAA pattern during the CESA. In order to investigate the self-assembly process, a range of pH values (1.0, 3.0, 5.0, 7.0) around pK_a, with a fixed concentration of 0.2 mg/mL PAA, were used with results shown in Figure 2 B,G–I. The values of the *H*, the *W*, and the *D* for Figure 2D–G are 20 nm, 4 μm, 24 μm for Figure 2D, 38 nm, 8 μm, 23 μm for Figure 2E, 30 nm, 10 μm, 5 μm for Figure 2F, and 80 nm, 8 μm, 20 μm for Figure 2G, respectively.

It was found that the morphology of the PAA rings tends to become disordered upon increasing the pH value above pK_a of PAA aqueous solution (Figure 2H–I). Similar results were also found in low concentrations of PAA from 0.05 to 0.4 mg/mL. The competition between pinning force and capillary force (depinning force) during the course of irreversible evaporation resulted in a controlled and repetitive "stick–slip" motion of contact line.[32] Hydrogen bonds were formed by the carboxylic acid groups (i.e., –COOH) in PAA aqueous solution and hydroxyl groups (i.e., –OH) on the silicon wafer substrate. Altogether, the interactions between the pinning force, the capillary force (depinning force), and the hydrogen bonds effectively resulted in the formation of PAA concentric rings. Increasing the pH value of PAA aqueous solution charged the uncharged carboxylic acid groups.[34] Due to the electrostatic repulsion among PAA chains, the chain conformation of PAA was changed from a shrunken random coil conformation to stretched random coil conformation. At the same time, some PAA was first deposited at the contact line; thus, there was electrostatic repulsion between deposited PAA and the other undeposited PAA which resulted in the disordered morphology. When the pH value was lower than the pK_a of PAA, the hydrogen bonds played a dominant role in the self-assembly process of the ring formation. However, at greater values of pH, electrostatic repulsion can lead to the formation of chaotic and random structures by the same procedure.

With the development of UV polymerization, SIPGP provided us with a convenient strategy to prepare polymer brushes even without a surface bound initiator on patterned SAMs, on carbon deposits, or with the direct use of a surface chemical contrast.[2] The photoactive group of –COOH on patterned PAA could be initiated to grow polymer brushes by SIPGP upon being immersed in various monomer solutions (for example, styrene) and irradiated with an UV lamp. Before SIPGP, the PAA pattern is nearly invisible (Figure 3A). After irradiation for an hour, the patterned polymer brushes were clearly visible to the naked eye (Figure 3B). Surface wettability was also investigated by measuring the water contact angle (CA) of the silicon patterned with concentric circles of PAA before and after SIPGP. The CA changed from 32° to 108° once the polystyrene (PS) brushes were formed on the patterned PAA rings, showing a drastic increase in hydrophobicity of the surface from the PS.

The difference in color observed by optical microscope was investigated further by AFM (Figure 4). The height of PAA rings generated from 0.05 mg/mL PAA aqueous solution was about 25 nm. Upon employing the SIPGP, a higher pattern of 50 nm was formed (Figure 4A,B). It was found that a significantly high PS brush could be obtained through this method by increasing the PAA concentration in the CESA process. Concentric rings with H of 900 nm could be achieved, compared to the original height of 60 nm, if a 0.1 mg/mL PAA

dx.doi.org/10.1021/la500996a | *Langmuir* 2014, 30, 4863–4867

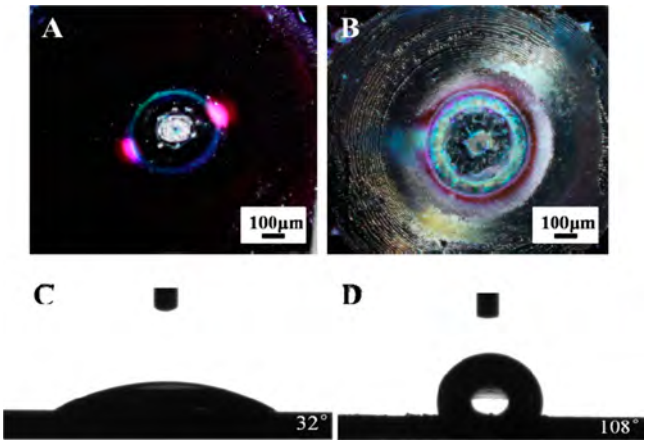

Figure 3. Optical micrograph images of silicon substrate patterned with PAA concentric rings (A) and with PS brushes after the SIPGP (B). Static water contact angle measurements (C) for A, and (D) for B.

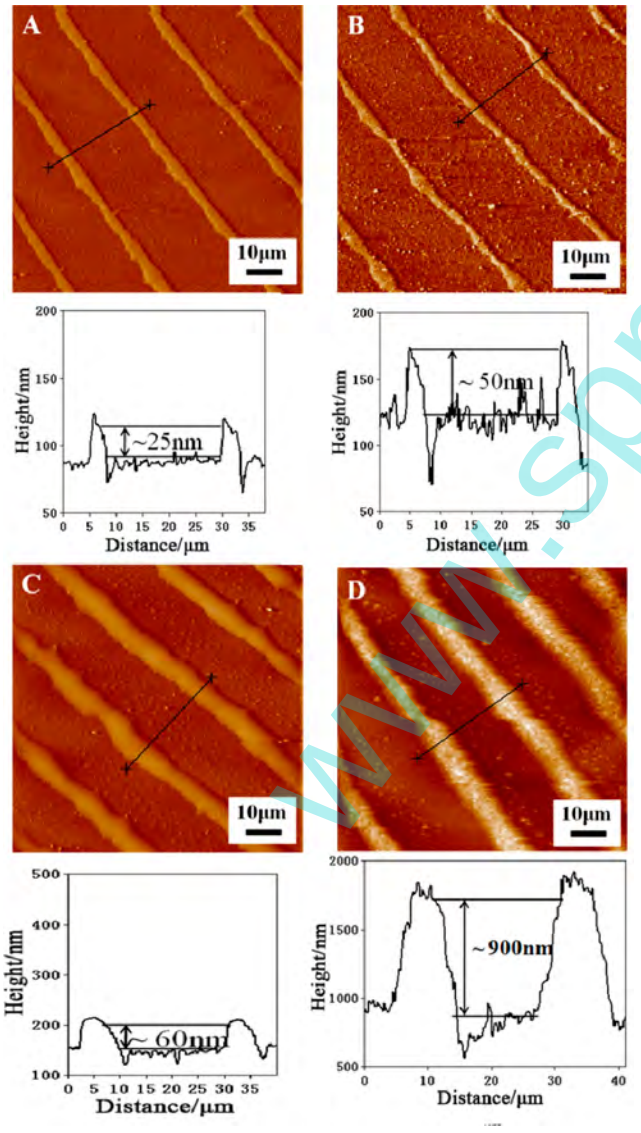

Figure 4. Representative AFM height images and corresponding profiles of before (A, C) and after (B, D) SIPGP of PAA concentric rings.

aqueous solution was used (Figure 4C,D). Further increasing the original concentration of PAA solution resulted in PS brushes that were several micrometers thick after SIPGP. However, the height was already beyond the characterization limit of AFM. Further detailed investigations of the polymerized PAA patterns are still in progress.

More recently, freestanding films have received continuing interest due to their potential applications in microsensors or actuators.[31,35] We showed that the PS brushes could be further released from the silicon surface by immersing the substrate in an aqueous KOH solution. The floating transparent film in centimeter size scale was easily observed by the naked eye (Figure 5A), and easily transferred onto another silicon surface

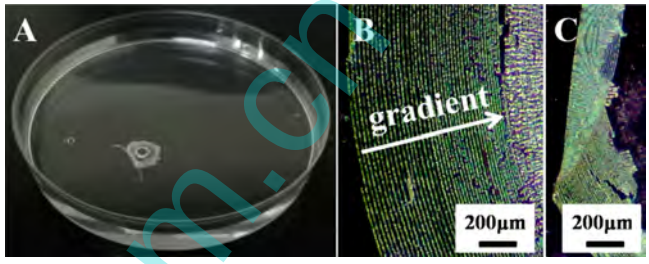

Figure 5. Freestanding film after etching with sodium hydroxide. (A) The whole freestanding film floating on the surface of water. (B) Part of the freestanding film showing gradient PAA rings. (C) Part of the freestanding film showing a scored film.

for optical measurements (Figure 5B,C). The resulting freestanding composite films, or as polymer carpet, not only have well-defined patterns, but also have precise overall dimensions.

■ CONCLUSIONS

In summary, we utilized a new and simple approach to create patterned polymer brushes without the necessity of sophisticated instruments. There are only two very easy steps. First, a poly(acrylic acid) photoactive template was formed by controlled evaporative self-assembly in a confined geometry. The size of photoactive template was on a large scale, up to a centimeter. Second, the photoactive template can be directly used for growth of polymer brushes by self-initiated photografting and photopolymerization. The morphology of obtained patterned polymer brushes such as the height of polymer brushes rings and periodic concentric rings was finely tuned by controlling the concentrations and pH of PAA aqueous solution. Furthermore, the freestanding patterned polymer brushes film can be easily peeled off for practical applications. The patterned polymer brushes or subsequent freestanding polymer carpets resulted from our simple and robust strategy may have the potentials in sensors and actuators or in other fields.

■ AUTHOR INFORMATION

Corresponding Authors

*E-mail: chenjing@nimte.ac.cn (J.C.).
*E-mail: tao.chen@nimte.ac.cn (T.C.).

Notes

The authors declare no competing financial interest.

dx.doi.org/10.1021/la500996a | Langmuir 2014, 30, 4863−4867

■ ACKNOWLEDGMENTS

This research was supported by the Chinese Academy of Science for Hundred Talents Program, the Chinese Central Government for Thousand Young Talents Program, and the Natural Science Foundation of China (51303195).

■ REFERENCES

(1) Zhao, B.; Brittain, W. J. Polymer brushes: Surface-immobilized macromolecules. *Prog. Polym. Sci.* **2000**, *25*, 677−710.
(2) Chen, T.; Amin, I.; Jordan, R. Patterned polymer brushes. *Chem. Soc. Rev.* **2012**, *41*, 3280−3296.
(3) Zhang, N.; Pompe, T.; Amin, I.; Luxenhofer, R.; Werner, C.; Jordan, R. Tailored poly(2-oxazoline) polymer brushes to control protein adsorption and cell adhesion. *Macromol. Biosci.* **2012**, *12*, 926−936.
(4) Schmelmer, U.; Jordan, R.; Geyer, W.; Eck, W.; Gölzhäuser, A.; Grunze, M.; Ulman, A. Surface-initiated polymerization on self-assembled monolayers: Amplification of patterns on the micrometer and nanometer scale. *Angew. Chem., Int. Ed.* **2003**, *42*, 559−563.
(5) Zhou, F.; Zheng, Z.; Yu, B.; Liu, W.; Huck, W. T. S. Multicomponent polymer brushes. *J. Am. Chem. Soc.* **2006**, *128*, 16253−16258.
(6) Ahn, S. J.; Kaholek, M.; Lee, W.-K.; LaMattina, B.; LaBean, T. H.; Zauscher, S. Surface-initiated polymerization on nanopatterns fabricated by electron-beam lithography. *Adv. Mater.* **2004**, *16*, 2141−2145.
(7) Ballav, N.; Schilp, S.; Zharnikov, M. Electron-beam chemical lithography with aliphatic self-assembled monolayers. *Angew. Chem., Int. Ed.* **2008**, *47*, 1421−1424.
(8) Beyer, A.; Godt, A.; Amin, I.; Nottbohm, C. T.; Schmidt, C.; Zhao, J.; Golzhauser, A. Fully cross-linked and chemically patterned self-assembled monolayers. *Phys. Chem. Chem. Phys.* **2008**, *10*, 7233−7238.
(9) Zhou, X.; Wang, X.; Shen, Y.; Xie, Z.; Zheng, Z. Fabrication of arbitrary three-dimensional polymer structures by rational control of the spacing between nanobrushes. *Angew. Chem., Int. Ed.* **2011**, *50*, 6506−6510.
(10) Nguyen, V. X.; Stebe, K. J. Patterning of small particles by a surfactant-enhanced Marangoni-Bénard instability. *Phys. Rev. Lett.* **2002**, *88*, 164501.
(11) Pauliac-Vaujour, E.; Stannard, A.; Martin, C.; Blunt, M.; Notingher, I.; Moriarty, P.; Vancea, I.; Thiele, U. Fingering instabilities in dewetting nanofluid. *Phys. Rev. Lett.* **2008**, *100*, 176102.
(12) Hu, H.; Larson, R. G. Marangoni effect reverses coffee-ring depositions. *J. Phys. Chem. B* **2006**, *110*, 7090−7094.
(13) Lin, Z. Controlled evaporative assembly of polymers from confined solutions. *J. Polym. Sci., Part B* **2010**, *48*, 2552−2557.
(14) Yabu, H.; Shimomura, M. Preparation of self-organized mesoscale polymer patterns on a solid substrate continuous pattern formation from a receding meniscus. *Adv. Funct. Mater.* **2005**, *15*, 575−581.
(15) Abkarian, M.; Nunes, J.; Stone, H. A. Colloidal crystallization and banding in a cylindrical geometry. *J. Am. Chem. Soc.* **2004**, *126*, 5978−5979.
(16) Lin, Z.; Granick, S. Patterns formed by droplet evaporation from a restricted geometry. *J. Am. Chem. Soc.* **2005**, *127*, 2816−2817.
(17) Harris, D. J.; Lewis, J. A. Marangoni effects on evaporative lithographic patterning of colloidal films. *Langmuir* **2008**, *24*, 3681−3685.
(18) Xu, J.; Xia, J.; Hong, S. W.; Lin, Z.; Qiu, F.; Yang, Y. Self-assembly of gradient concentric rings via solvent evaporation from a capillary bridge. *Phys. Rev. Lett.* **2006**, *96*, 066104.
(19) Xu, J.; Xia, J.; Lin, Z. Evaporation-induced self-assembly of nanoparticles from a sphere-on-flat geometry. *Angew. Chem., Int. Ed.* **2007**, *46*, 1860−1863.
(20) Hong, S. W.; Byun, M.; Lin, Z. Robust self-assembly of highly ordered complex structures by controlled evaporation of confined microfluids. *Angew. Chem., Int. Ed.* **2009**, *48*, 512−516.
(21) Han, W.; Byun, M.; Zhao, L.; Rzayev, J.; Lin, Z. Controlled evaporative self-assembly of hierarchically structured bottlebrush block copolymer with nanochannels. *J. Mater. Chem.* **2011**, *21*, 14248−14253.
(22) Li, B.; Han, W.; Byun, M.; Zhu, L.; Zou, Q.; Lin, Z. Macroscopic highly aligned DNA nanowires created by controlled evaporative self-assembly. *ACS Nano* **2013**, *7*, 4326−4333.
(23) Han, W.; Byun, M.; Lin, Z. Assembling and positioning latex nanoparticles via controlled evaporative self-assembly. *J. Mater. Chem.* **2011**, *21*, 16968−16972.
(24) Han, W.; He, M.; Byun, M.; Li, B.; Lin, Z. Large-scale hierarchically structured conjugated polymer assemblies with enhanced electrical conductivity. *Angew. Chem., Int. Ed.* **2013**, *52*, 2564−2568.
(25) Byun, M.; Han, W.; Li, B.; Xin, X.; Lin, Z. An unconventional route to hierarchically ordered block copolymers on a gradient patterned surface through controlled evaporative self-assembly. *Angew. Chem., Int. Ed.* **2013**, *52*, 1122−1127.
(26) Byun, M.; Han, W.; Li, B.; Hong, S. W.; Cho, J. W.; Zou, Q.; Lin, Z. Guided organization of λ-DNA into microring arrays from liquid capillary bridge. *Small* **2011**, *7*, 1641−1646.
(27) Kim, T. Y.; Kwon, S. W.; Park, S. J.; Yoon, D. H.; Suh, K. S.; Yang, W. S. Self-organized graphene patterns. *Adv. Mater.* **2011**, *23*, 2734−2738.
(28) Steenackers, M.; Kuller, A.; Stoycheva, S.; Grunze, M.; Jordan, R. Structured and gradient polymer brushes from biphenylthiol self-assembled monolayers by self-initiated photografting and photopolymerization (SIPGP). *Langmuir* **2009**, *25*, 2225−2231.
(29) Chen, J.; Xiao, P.; Gu, J.; Han, D.; Zhang, J.; Sun, A.; Wang, W.; Chen, T. A smart hybrid system of Au nanoparticle immobilized PDMAEMA brushes for thermally adjustable catalysis. *Chem. Commun.* **2014**, *50*, 1212−1214.
(30) Xiao, P.; Gu, J.; Chen, J.; Han, D.; Zhang, J.; Cao, H.; Xing, R.; Han, Y.; Wang, W.; Chen, T. A microcontact printing induced supramolecular self-assembled photoactive surface for patterning polymer brushes. *Chem. Commun.* **2013**, *49*, 11167−11169.
(31) Amin, I.; Steenackers, M.; Zhang, N.; Beyer, A.; Zhang, X.; Pirzer, T.; Hugel, T.; Jordan, R.; Golzhauser, A. Polymer carpets. *Small* **2010**, *6*, 1623−1630.
(32) Shmuylovich, L.; Shen, A. Q.; Stone, H. A. Surface morphology of drying latex films: multiple ring formation. *Langumir* **2002**, *18*, 3441−3445.
(33) Han, W.; Lin, Z. Learning from "coffee rings": Ordered structures enabled by controlled evaporative self-assembly. *Angew. Chem., Int. Ed.* **2012**, *51*, 1534−1546.
(34) Choi, J.; Rubner, M. F. Influence of the degree of ionization on weak polyelectrolyte multilayer assembly. *Macromolecules* **2005**, *38*, 116−124.
(35) Amin, I.; Steenackers, M.; Zhang, N.; Schubel, R.; Beyer, A.; Golzhauser, A.; Jordan, R. Patterned polymer carpets. *Small* **2011**, *7*, 683−687.